Article

Unexpected Effects of K and Adenosine Triphosphate on the Thermal Stability of Na,K-ATPase

M Agueda Placenti, Sergio Benjamín Benjamin Kaufman, F
Luis Gonzalez Flecha, and Rodolfo Martín González-Lebrero

Just Accepted

1
2
3
4
5
6
7
8
9
10
11
12
13
14
15
16
17
18
19
20
21
22
23
24
25
26
27
28
29
30
31
32
33
34
35
36
37
38
39
40
41
42
43
44
45
46
47
48
49
50
51
52
53
54
55
56
57
58
59
60

Unexpected Effects of K$^+$ and Adenosine Triphosphate on the Thermal Stability of Na$^+$,K$^+$- ATPase

M. Agueda Placenti; Sergio B. Kaufman; F. Luis González Flecha and Rodolfo M. González-Lebrero[*]

Instituto de Química y Fisicoquímica Biológicas and Departamento de Química Biológica, Facultad de Farmacia y Bioquímica. Universidad de Buenos Aires - CONICET. Buenos Aires, Argentina

ABSTRACT: Na^+,K^+-ATPase is an integral membrane protein which couples ATP hydrolysis to the transport of three Na^+ out and two K^+ into the cell. The aim of this work is to characterize the effect of K^+, ATP and Mg^{2+} (essential activator) on the Na^+,K^+-ATPase thermal stability. In all conditions tested, thermal inactivation of the enzyme is concomitant with a structural change involving the ATP binding site and membrane-associated regions. Both ligands exert a clear stabilizing effect due to both enthalpic and entropic contributions. Competition experiments between ATP and K^+ showed that when ATP is present, the inactivation rate coefficient exhibits a biphasic dependence on K^+ concentration. At low $[K^+]$ destabilization of the enzyme is observed, while stabilization occurred at larger cation concentrations. This is not expected for a simple competition between the enzyme and two ligands that individually protect the enzyme. A model that includes enzyme species with none, one or two K^+ and/or one molecule of ATP bound explain the experimental data. We concluded that despite both ligands stabilize the enzyme, the species with one K^+ and one ATP simultaneously bound is unstable.

INTRODUCTION

Na^+,K^+-ATPase is an integral membrane protein that couples ATP hydrolysis to the active transport of three Na^+ ions out and two K^+ ions into the cell.[1] Similarly to other ATPases, enzyme activity requires the presence of Mg^{2+} as the complex ATP.Mg is postulated to be the true substrate of the enzyme.[2,3] The minimum functional unit is a heterodimer composed of a large catalytic α subunit (1016 residues) and a smaller β subunit (302 residues) with regulatory functions.[4,5] The α subunit has three characteristic cytoplasmic domains -actuator (A), nucleotide-binding (N) and phosphorylation (P) domains- together with a transmembrane domain, formed by 10 helical segments, which includes the cation transport sites.[6–8]

The working cycle of the enzyme includes: i) binding of ATP ii) formation and breakdown of a phosphoenzyme intermediary, iii) conformational changes between two main conformational states -the so called E_1 and E_2 conformers- and iv) occlusion/ deocclusion of Na^+ and K^+ ions.[9,10] The E_1 conformer is the main enzyme specie in the presence of Na^+, ATP or Mg^{2+} whereas K^+ shifts the equilibrium towards E_2.[11,12] In the absence of ATP, Na^+ and Mg^{2+}, two K^+ ions are occluded in the E_2 conformer ($E_2(K_2)$).[9,10,13–15] When ATP is present, deocclusion of K^+ is accelerated, leading to E_1.ATP. Biochemical and biophysical evidences support the idea that the structure of the enzyme in $E_2(K_2)$ is rather different from that in E_1.[6,16–21]

Thermal inactivation has been used as a tool to study protein interactions and domain structure of the Na^+,K^+-ATPase and other related ATPases.[22–26] Additionally, some studies have described the influence of natural ligands of the enzyme on its thermal inactivation.[27,28] Our previous results showed that K^+ or Rb^+ stabilize the enzyme, while Na^+ produce a decrease in the Na^+,K^+-ATPase stability.[29] Both effects are exerted by specific binding of these cations to the pump

independently of the ionic strength effect. Also, we provided strong evidence that Rb^+ (or K^+) stabilizing effect is due to the occlusion of these cations into the enzyme.

In this work, we will characterize the effect of ATP and Mg^{2+} by evaluating functional and structural properties of the protein. Further analysis according to the Transition State Theory will be performed in order to obtain the thermodynamic activation parameters for the inactivation process in the absence or presence of the ligands. In addition, the combined effect of ATP and K^+ will also be characterized, proposing a minimal model to explain their interactions.

MATERIALS AND METHODS

Enzyme. Na^+,K^+-ATPase partially purified from pig kidney outer medulla according to the procedure of Jensen et al. was kindly provided by the Department of Biophysics of the University of Århus, Denmark. [30,31] The specific activity of the preparation in optimal conditions (150 mM NaCl, 20 mM KCl, 3 mM ATP, 4 mM $MgCl_2$, and 25 mM imidazole−HCl, pH 7.4) was 30.8 μmol Pi min^{-1} (mg protein)$^{-1}$ at 37 °C.

Reagents. ATP disodium salt from Sigma was dissolved in Tris 200 mM (pH 7.4) and subjected to cation exchange chromatography (AG MP-50, BioRad) to remove Na^+, replacing it with Tris. All other reagents were of analytical grade.

Thermal Inactivation. Thermal inactivation experiments were performed as previously described, mixing a volume of the enzyme suspension (75 μg/ml) with 1.5 volumes of a solution equilibrated at the working temperature.[29] Preincubation temperatures were set between 52 to 60 ºC and controlled within a range of ± 0.1 ºC. The preincubation media contained EDTA 0.25 mM and Tris 25 mM (pH 6.2 ± 0.1 at each temperature) and, or not, Mg^{2+}, ATP and K^+ (see Results). After preincubation, the reaction tubes were placed in an ice-water bath to rapidly drop

the temperature and stop the inactivation reaction and then left for 3-5 min. The tubes were then placed in a 25 ºC bath for 10 min prior to the determinations.

Determination of Na$^+$,K$^+$-ATPase Activity. After preincubation Na$^+$,K$^+$-ATPase activity was measured by incubating the enzyme (15 µg/ml) for different time periods at 25 ºC. Independently of the preincubation media composition, ATPase activity was measured in a media supplemented to a final composition of 150 mM NaCl, 20 mM KCl, 3 mM ATP, 4 mM MgCl2, 0.25 mM EDTA and 25 mM Tris-HCl (pH 7.4 at 25 ºC). Incubation times were short enough to ensure initial rate conditions.

The amount of Pi released from ATP hydrolysis was determined according to the method described by Baginski et al. with some modifications.[32,33] 250 µL of reaction media were mixed with an equal volume of reagent A (composed by 0.5% w/v ammonium heptamolybdate and 3% w/v ascorbic acid in 0.5 N HCl at approximately 4 °C) stopping the enzymatic reaction. The resulting mixture was incubated in an ice-water bath for 20 minutes, after which 500 µL of reagent B (composed by 2% w/v sodium citrate, 2% w/v sodium arsenite and 2% v/v acetic acid) were added and the tubes were incubated at 37 °C for 20 minutes. Finally, after approximately 30 minutes at room temperature absorbance at 850 nm was recorded.

Fluorescence Measurements. Steady state fluorescence measurements were performed using a Jasco FP-6500 spectrofluorometer with a 3 mm quartz cuvette thermostated at 25 °C. Emission spectra of Na$^+$,K$^+$-ATPase (30µg/ml, abs$_{280nm}$= 0.170) were recorded between 305 and 450 nm after excitation at 295 nm in the same media used in the inactivation procedure. Both excitation and emission bandwidths were set at 3 nm. The spectra were corrected for background emission (without enzyme). Eosin-Y fluorescence was measured after mixing the protein with the probe to a final concentration of 0.23 µM (abs$_{517nm}$= 0.044) except when indicated. Emission spectra were

recorded between 530 and 640 nm after excitation at 520 nm. Total intensity (I_t) was calculated as the sum of fluorescence intensities recorded at each wavelength.

Transition State Theory Analysis. In a viscous solvent, the variation of the inactivation rate coefficient with temperature can be described by Kramers model, [34–39] as follows:

$$k = \nu \, \frac{\eta_0}{\eta_T} \, e^{-\frac{\Delta G^{\ddagger}}{R\,T}} \tag{1}$$

where ν represents the k value at the reference temperature for a barrierless process, η is the medium viscosity either at the reference temperature (η_0) or at the preincubation temperature (η_T), and $\Delta G^{\ddagger}$ is the activation free energy. We employed a reference temperature of 329 K (56ºC) and ν was fixed at 10^6 s^{-1}, which is considered a reasonable consensus value.[40,41] $\Delta G^{\ddagger}$ can be expressed in terms of activation enthalpy ($\Delta H^{\ddagger}$) and entropy ($\Delta S^{\ddagger}$),

$$\Delta G^{\ddagger} = \Delta H^{\ddagger} - T\,\Delta S^{\ddagger} \tag{2}$$

Thus, the variation of k with preincubation temperature as a function of $\Delta H^{\ddagger}$ and $\Delta S^{\ddagger}$ could be obtained by replacing eq 2 into 1.

$$k = \nu \, \frac{\eta_0}{\eta_T} \, e^{-\frac{\Delta H^{\ddagger}}{R\,T}} \, e^{\frac{\Delta S^{\ddagger}}{R}} \tag{3}$$

Data Analysis. Equations were fitted to the experimental data by nonlinear regression. Best fitting values of the parameters are expressed as mean ± standard error. Statistical weights were 1/(standard error)^2 in all cases where an equation was fitted to the inactivation rate coefficient values.

Model Selection. In order to evaluate the goodness of fit of a given equation to the experimental results and to choose among different models, we used the AIC_C criterion which is defined as AIC_C = N. ln (SS) + 2 N P/(N-P-1), with N = number of data, P = number of

parameters plus 1, and SS = sum of weighted square residual errors.[42] The best equation was considered that which gave the lower value of AIC.

RESULTS

The Whole Conformation of Na$^+$,K$^+$-ATPase is Disrupted during Thermal Inactivation. Thermal inactivation experiments were performed as detailed in material and methods, preincubating the enzyme for different time periods at 53.5 °C and then measuring Na$^+$,K$^+$-ATPase activity (Figure 1A). Simultaneously, structural changes on the Na$^+$,K$^+$-ATPase due to thermal inactivation were evaluated by measuring tryptophan fluorescence according to the previously described procedure (Figure 1B).[29] This technique is well known as a powerful tool to monitor changes in protein tertiary structure.[43] Additionally, ATP binding site integrity during thermal inactivation was evaluated by measuring eosin-Y binding (Figure 1C). This molecule is a fluorescence probe that binds noncovalently to the ATP binding site, competing with the nucleotide (Figure S1).[44,45] Fluorescence spectra were recorded after addition of eosin-Y to the enzyme preincubated for different time periods (Inset in Figure 1C).
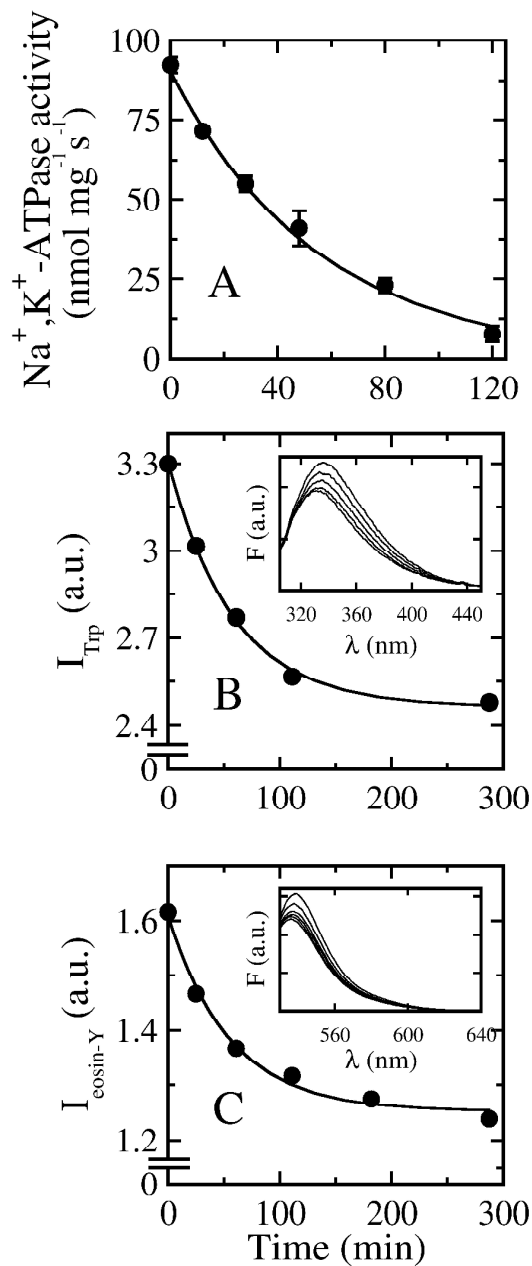
Figure 1. Na$^+$,K$^+$-ATPase thermal inactivation and associated structural changes. Na$^+$,K$^+$-ATPase activity (Panel A), Trp fluorescence intensity (Panel B) or eosin-Y fluorescence intensity (Panel C) were registered after different preincubation time periods at 53.5 °C. Continuous line is a plot of eq 4 with the best fitting values of k, M_0 and M_∞. Insets in panels B and C show the corresponding Trp or eosin-Y fluorescence spectra recorded.

As previously described,[29] enzyme activity and tryptophan fluorescence decay with preincubation time following a single exponential function of time at a given temperature (eq 4) which is indicative of a one-step process. Furthermore, eosin-Y fluorescence decay can also be described by the same equation.

$$M_t = \left(M_0 - M_\infty\right) e^{-kt} + M_\infty \tag{4}$$

where M_t is the measure performed at preincubation time (t), M_0 and M_∞ are the values of the measure at t = 0 or tending to infinity, respectively, and k is the thermal inactivation rate coefficient. Notice that, in the case of Na^+,K^+-ATPase activity measurements, M_∞ was equal to zero since complete inactivation was observed at long preincubation time periods.

It is worth noting that the inactivation rate coefficients (k) obtained by measuring enzyme activity were not significantly different from those obtained by either tryptophan or eosin-Y fluorescence measurements at the same temperature (i.e. at 53.5 ºC $k = (3.0 \pm 0.2).10^{-4}$ s^{-1} for Na^+,K^+-ATPase activity, $(2.9 \pm 0.2).10^{-4}$ s^{-1} for Trp fluorescence and $(3.0 \pm 0.4).10^{-4}$ s^{-1} for eosin-Y fluorescence). This results suggest that enzyme properties measured would be reflecting the same phenomenon in which the structural changes observed and the loss in ATP binding capacity are concomitant whit the enzyme inactivation process.

ATP and Mg^{2+} Protect Na^+, K^+-ATPase against Thermal Inactivation. The effects of ATP or Mg^{2+} were evaluated by measuring the remaining Na^+,K^+-ATPase activity after preincubation of the enzyme for different time periods in media containing several ligand concentrations. In all cases, thermal inactivation process was described by a single exponential function of time (eq 4) and the inactivation rate coefficient (k) was obtained. Figure 2 shows the best fitting values of k as a function of the concentration of ATP (Panel A) or Mg^{2+} (Panel B). It can be seen that as ligand concentration increases, the values of k decrease up to a constant value. This result

indicates that both ATP and Mg^{2+} exert a stabilizing effect upon the enzyme thermal inactivation. The dependence of k with ligand concentration can be phenomenologically described by a decreasing hyperbola plus an independent term (a kinetic model is included in the Discussion section).

$$k = \frac{(k_0 - k_\infty) K_{0.5}}{K_{0.5} + [X]} + k_\infty \qquad (5)$$

where [X] represents the ligand concentration -i.e. [ATP] or $[Mg^{2+}]$-, k_0 and k_∞ the thermal inactivation rate coefficients in the absence of ligand or when the ligand concentration tends to infinite respectively, and $K_{0.5}$ the ligand concentration at which k is equal to the average of k_0 and k_∞.
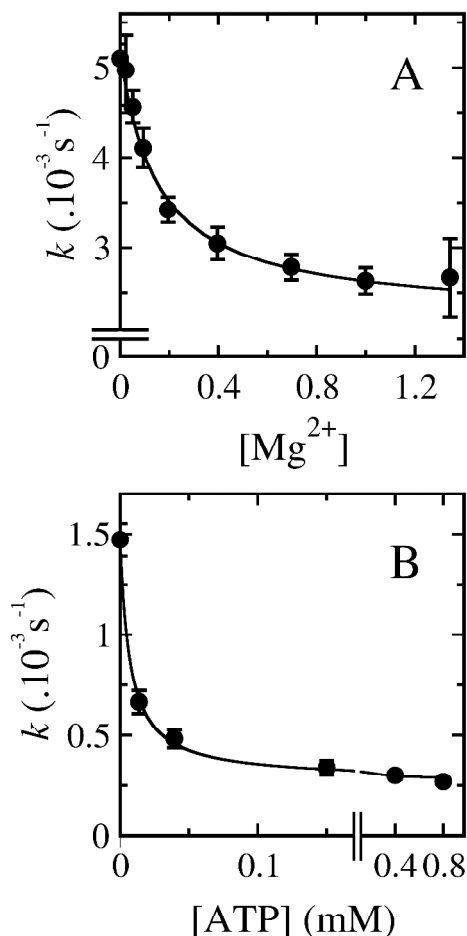
Figure 2. Effect of ATP or Mg^{2+} on the Na^+,K^+-ATPase thermal inactivation. The enzyme was preincubated during several time periods in the presence of different concentrations of ATP at 56.8 °C or Mg^{2+} at 58.5 °C. Inactivation rate coefficients (k) were obtained by fitting eq 4 to the time courses of the remaining Na^+,K^+-ATPase activity, and represented as a function of $[Mg^{2+}]$ (Panel A) or [ATP] (Panel B). It is important to note that less than 0.5 % of ATP was hydrolysed after 1 hour preincubation. Continuous lines are plots of eq 5 with the best fitting values of k_0, k_∞ and $K_{0.5}$ for ATP or Mg^{2+}.

The protective effect of these ligands on the Na^+,K^+-ATPase thermal inactivation was further evaluated by performing inactivation experiments at different preincubation temperatures (in the range of 52-60 ºC). The single exponential behavior observed in all time course experiments led us to postulate that inactivation of the enzyme occurs through a single step reaction involving two enzyme states -active and inactive-, implying the existence of a unique transition state. Either in the absence of ligands (Figure 3A) or in the presence of 2 mM ATP or 1 mM Mg^{2+} (Figure 3B and 3C, respectively) it can be observed that the values of k increase exponentially with preincubation temperature. The linear Arrhenius plots (Insets in Figure 3) indicate that, in the temperature range evaluated, the change in activation heat capacity ($\Delta Cp^{\ddagger}$) is approximately equal to zero.
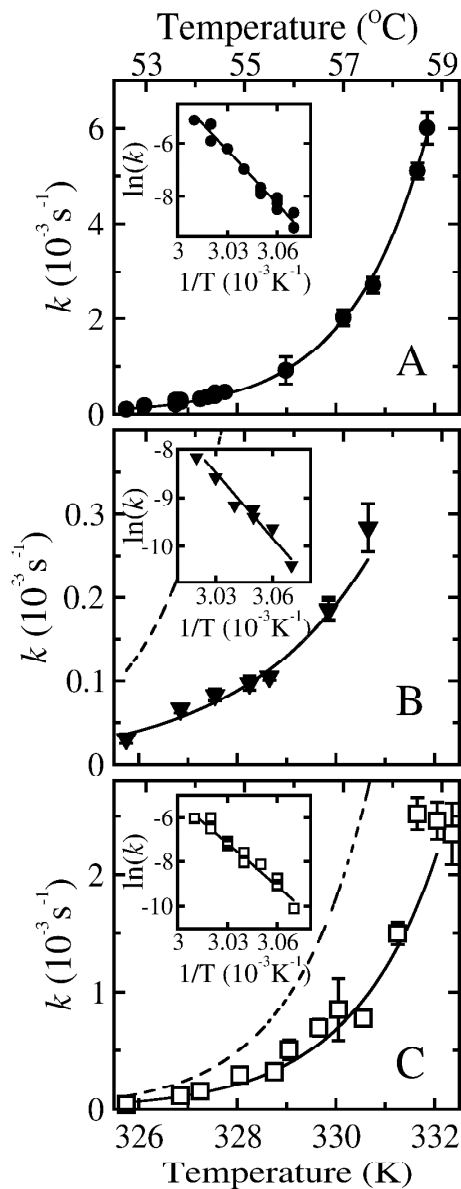
Figure 3. Temperature dependence of thermal inactivation of Na^+,K^+-ATPase in the presence of ATP or Mg^{2+}. Values of inactivation rate coefficients k were obtained by fitting eq 4 to inactivation time course experiments performed at different preincubation temperatures in the absence of ligands (Panel A,●), or in the presence of 2 mM ATP (Panel B,▼) or 1 mM Mg^{2+} (Panel C, □). Continuous lines are plots of eq 3 with the best fitting values of $\Delta H^{\ddagger}$ and $\Delta S^{\ddagger}$ shown in Table 1. Dashed lines in Panels B and C are plots of eq 3 fitted to the data in Panel A. Insets show the corresponding Arrhenius plots.

A Kramers model was used to analyze the variation of the reaction rate coefficient (k) with temperature in a viscous solvent (see Material and Methods). Fitting of eq 3 to the values of k (continuous lines in Figure 4) allowed us to obtain the thermodynamic activation parameters for the thermal inactivation process ($\Delta G^{\ddagger}$, $\Delta H^{\ddagger}$, and $\Delta S^{\ddagger}$) in each experimental preincubation condition (Table 1). To complete a quantitative comparison between the stabilizing properties of different ligands, we also evaluated the effect of the addition of 40 mM K^{+} to the preincubation media used in this work (Figure 4 and Table 1), knowing that this cation protects the enzyme against thermal inactivation. [28,29,46]
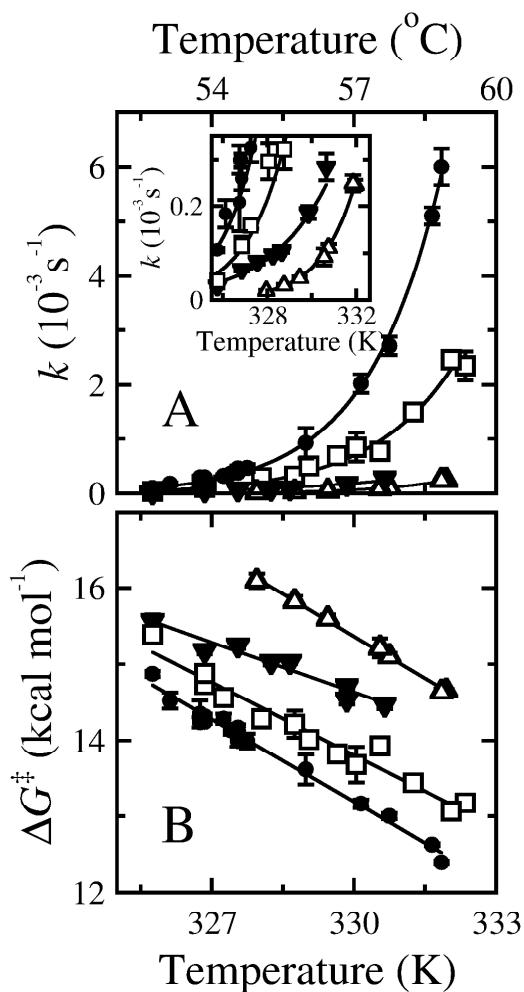
Figure 4. Kramers analysis of the effect of ATP, Mg^{2+} or K^+ on the temperature dependencies of thermal inactivation of Na^+,K^+-ATPase. Panel A shows k values obtained by fitting eq 4 to inactivation experiments performed at different preincubation temperatures in the absence of ligands (●), or in the presence of 2 mM ATP (▼), 1 mM Mg^{2+} (□) or 40 mM K^+ (Δ). Continuous lines are plots of eq 3 with the best fitting values of $\Delta H^{\ddagger}$ and $\Delta S^{\ddagger}$ shown in Table 1. Panel B shows $\Delta G^{\ddagger}$ values obtained by fitting eq 1 to each inactivation experiment. Continuous lines in Panel B are plots of eq 2 with the best fitting values of $\Delta H^{\ddagger}$ and $\Delta S^{\ddagger}$ shown in Table 1.

Table 1. Inactivation Rate Coefficient and Thermodynamic Activation Parameters at 56 ºC

	Without ligands	Mg^{2+}	ATP	K^+
k $(.10^{-4}$ $s^{-1})$	10 ± 1	4.3 ± 0.7	1.3 ± 0.1	0.39 ± 0.04
$\Delta G^{\ddagger}$ (kcal.mol^{-1})	13.52 ± 0.07	14.10 ± 0.08	14.86 ± 0.06	15.66 ± 0.07
$\Delta H^{\ddagger}$ (kcal.mol^{-1})	134 ± 3	122 ± 5	86 ± 7	139 ± 3
T.$\Delta S^{\ddagger}$ (kcal.mol^{-1})	120 ± 3	108 ± 5	71 ± 7	123 ± 3

For all ligands tested it can be seen that the activation free energy at a reference temperature slightly change as a result of large changes in both entropic and enthalpic components (Table 1). Even though ATP and Mg^{2+} showed a stabilizing effect in the temperature range evaluated, the change on $\Delta G^{\ddagger}$ promoted by ATP ($\Delta\Delta G^{\ddagger}$ = 1.34 kcal/mol) is higher than in the case of Mg^{2+} ($\Delta\Delta G^{\ddagger}$ = 0.58 kcal/mol). Nevertheless, it is remarkable that the protection afforded by these ligands is less than that produced by the binding/occlusion of K^+ ($\Delta\Delta G^{\ddagger}$ = 2.14 kcal/mol) indicating that the occluded state of the enzyme is the most stable species.

The E and EKATP Intermediates of the Na^+,K^+-ATPase are the Less Stable Species. Thermal inactivation experiments were performed at 56.8 °C after the addition of different concentrations of both ATP (0 to 2.5 mM) and K^+ (0 to 10 mM) to the preincubation media.

Figure 5 shows the best fitting values of the inactivation rate coefficients (k) as a function of K$^+$

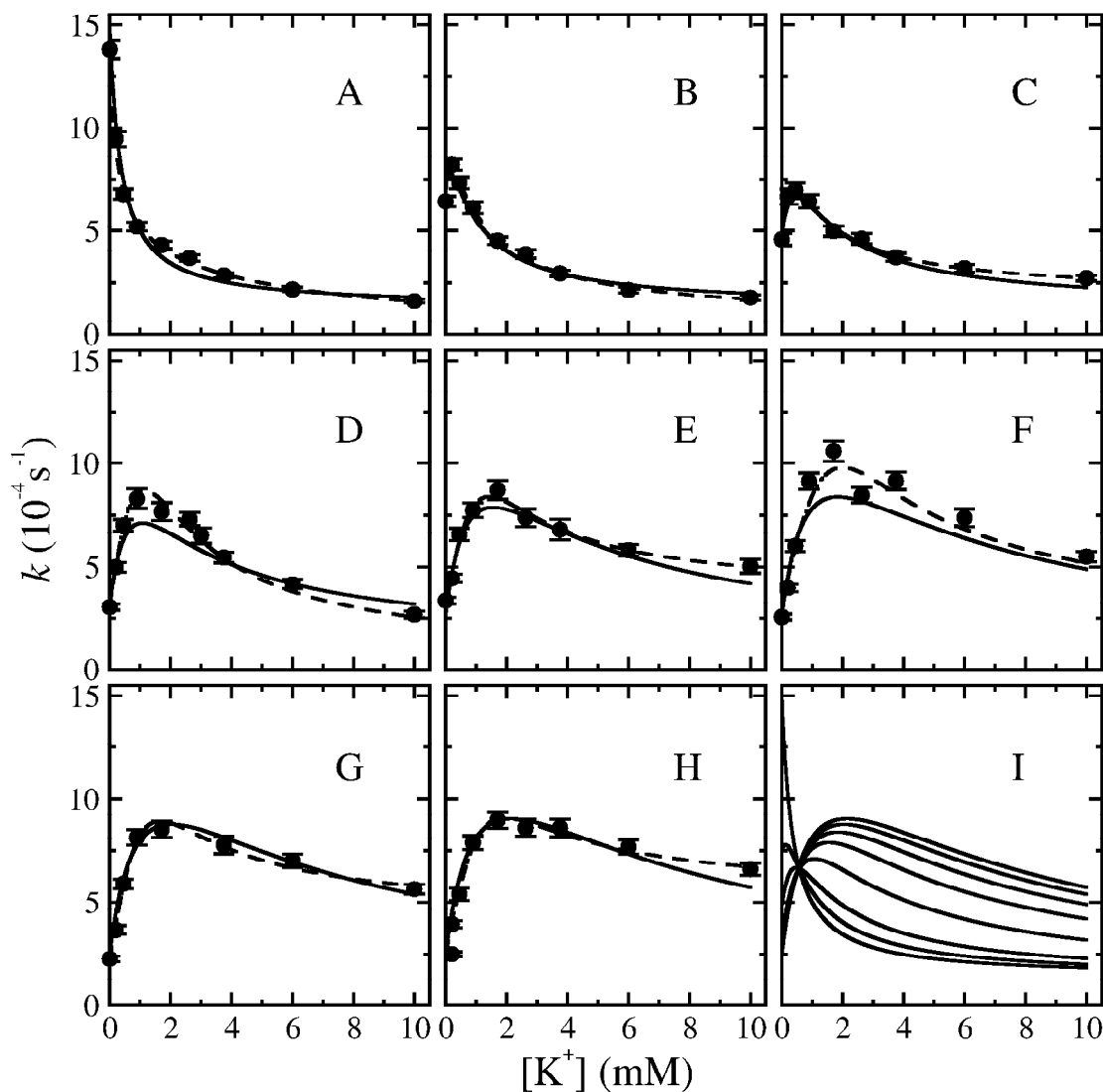concentration, where each panel corresponds to a different ATP concentration.

Figure 5. Effect of the simultaneous presence of K$^+$ and ATP on the Na$^+$,K$^+$-ATPase thermal

inactivation. Panels show the inactivation rate coefficient (k) obtained at 56.8 ºC as a function of

[K$^+$] for [ATP] 0 (Panel A), 0.014 (B), 0.04 (C), 0.15 (D), 0.40 (E), 0.80 (F), 1.5 (G) and 2.5 mM

(H) in the preincubation media. Dashed lines are plots of best minimal empirical equation (eq 6)

fitted to each data set. Continuous lines are plots of model-derived equation (eq 7) fitted to all the

experimental data simultaneously with the best fitting values showed in Table 3. Panel I shows

simulations of the model-derived equation as a function of $[K^+]$ for the ATP concentrations from Panels A-H using the best fitting values given in Table 3.

In the absence of the nucleotide (Figure 5A) k values decrease hyperbolically with the increment of K^+ concentration up to a constant value, as has been previously described under different experimental conditions.[29] However, even though both ATP and K^+ individually have shown a clear stabilizing effect on the Na^+,K^+-ATPase thermal inactivation, it can be seen that when both ligands are present in the preincubation media, and [ATP] is kept constant, the inactivation rate coefficient k shows a biphasic dependence on K^+ concentration. In the presence of ATP, k increases at low K^+ concentrations indicating destabilization of the enzyme and, conversely, when $[K^+]$ increase even more, a stabilizing effect can be observed. Also, the maximum value of k progressively shifts to higher $[K^+]$ as [ATP] increases (Figures 5 B-H).

If the same set of data is represented as a function of [ATP] at constant $[K^+]$ a simpler behavior is observed. Figure 6 shows a representative set of whole data shown in Figure S2.
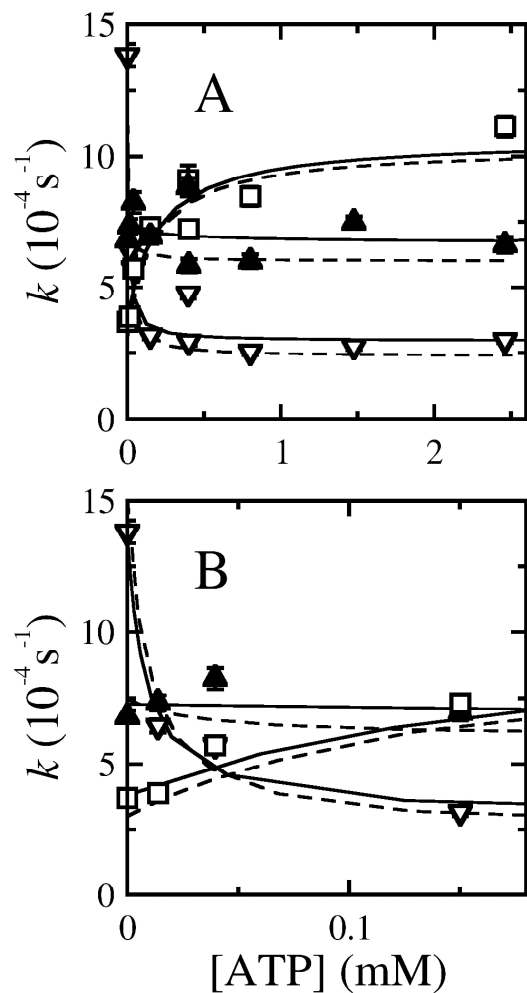
Figure 6. Effect of the simultaneous presence of K^+ and ATP on the Na^+, K^+-ATPase thermal inactivation. Panels show the inactivation rate coefficient (k) obtained at 56.8 ºC as a function of [ATP] for [K^+] 0 (∇), 0.45 (▲) or 3.7 (□) mM in the preincubation media. Dashed lines are plots of best minimal empirical equation (eq 6) fitted to each data set. Continuous lines are plots of model-derived equation (eq 7) fitted to all the experimental data simultaneously with the best fitting values showed in Table 3.

Depending on [K^+] in the preincubation media, ATP could either stabilize or destabilize the enzyme. At low [K^+] k values decrease with ATP concentration, whereas at higher [K^+] (0.9 to 10 mM) k increases. This curve could be described by hyperbolic functions of [ATP] at each

[K$^+$]. It can be observed that the [ATP] needed to produce a half-maximal effect on k, increases with the increment of [K$^+$].

In order to find a model able to describe the results of this section as a whole, we followed the procedure described by González-Lebrero et al..[47] Briefly, it consists of finding the minimal "empirical" equation that gives the best fit to the experimental data according to the AIC criterion, and from this function infer which states of the enzyme are actually present. For the first step, several quotients of two polynomial functions of [K$^+$] were fitted to the k values at each ATP concentration (Figure 5). The best minimal empirical equation was:

$$k = \frac{N_0 + N_1\,[K^+] + N_2\,[K^+]^2}{1 + D_1\,[K^+] + D_2\,[K^+]^2} \tag{6}$$

and the best fitting values for the coefficients N's and D's decrease hyperbolically with the increase of ATP concentration up to a constant value (Figure S3).

The terms of eq 6 and the hyperbolical dependence of k on ATP concentration indicate that the enzyme can bind/occlude one or two K$^+$ ions either with or without one ATP bound. Based on that, the possible states of the enzyme and the equilibria among them are shown in Scheme 1, where each species has its own inactivation rate coefficient and the inactivation process is in all cases irreversible.
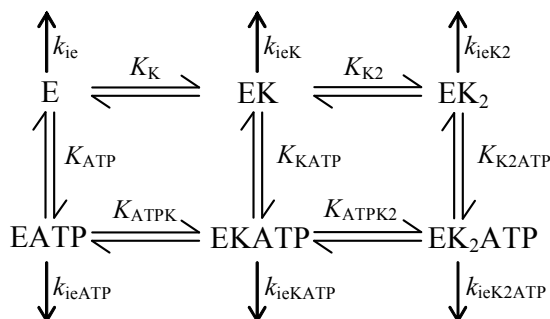
Scheme 1. Model of the interaction of the Na$^+$, K$^+$-ATPase with K$^+$ and ATP and the thermal inactivation constants.

According to Scheme 1 and considering rapid equilibrium for ligand binding, k is then defined as a function of both ATP and K^+ as:

$$k = \frac{N_{00} + N_{10}[K^+] + N_{20}[K^+]^2 + N_{01}[ATP] + N_{11}[ATP][K^+] + N_{21}[ATP][K^+]^2}{1 + D_{10}[K^+] + D_{20}[K^+]^2 + D_{01}[ATP] + D_{11}[ATP][K^+] + D_{21}[ATP][K^+]^2} \qquad (7)$$

where the N_{xx}'s and D_{xx}'s coefficients are defined in terms of Scheme 1 as shown in Table 2.

Note that at a constant ATP concentration eq 7 becomes equivalent to eq 6, whose coefficients are hyperbolic functions of [ATP] (Table S1). Conversely, at a constant $[K^+]$ eq 7 takes the form of a hyperbolic function of [ATP].

Table 2. **Meaning of the Coefficients from eq 7 in Terms of the Equilibrium and Thermal Inactivation Rate Constants from Scheme 1**

Coefficient	Meaning	Coefficient	Meaning
N_{00}	k_{ie}	D_{10}	K_K^{-1}
N_{10}	$K_K^{-1} k_{ieK}$	D_{20}	$K_K^{-1} K_{K2}^{-1}$
N_{20}	$K_K^{-1} K_{K2}^{-1} k_{ieK2}$	D_{01}	K_{ATP}^{-1}
N_{01}	$K_{ATP}^{-1} k_{ieATP}$	D_{11}	$K_{ATP}^{-1} K_{ATPK}^{-1}$
N_{11}	$K_{ATP}^{-1} K_{ATPK}^{-1} k_{ieATPK}$	D_{21}	$K_{ATP}^{-1} K_{ATPK}^{-1} K_{ATPK2}^{-1}$
N_{21}	$K_{ATP}^{-1} K_{ATPK}^{-1} K_{ATPK2}^{-1} k_{ieATPK2}$		

Equation 7 was then fitted to the k values as a function of both $[K^+]$ and [ATP] in order to obtain the constants defined in the model in scheme 1. The following constraints were included, provided that they did not affect the goodness of the fit (i.e. diminished the value of the AIC, see Materials and Methods): (a) Since, in absence of ATP k decreases hyperbolically with $[K^+]$, K_{K2} was fixed to be $4.K_K$ and $k_{ieK}=(k_{ie}+k_{ieK2})/2$. (b) As the value of k_{ieATPK} could not be obtained independently with enough precision, it was set to be equal to k_{ie}. This equivalence is justified because both rate constant values were similar when the constraint was not applied in the fitting. (c) Considering eq 6, when K^+ concentration tends to infinity, k tends to the ratio N_2/D_2. In this condition, the enzyme will be predominantly in the states with two K^+ occluded and either

without or with ATP bound (in absence or when [ATP] tends to infinity, respectively). Given

that this ratio does not significantly vary with ATP concentration, there would be no difference

between the inactivation rate constant of these species, and therefore the value of $k_{ieATPK2}$ was

fixed to that of k_{ieK2}. Table 3 shows the best fitting values of the constants from Scheme 1.

Notice that there is good agreement between the simulated values of the model-derived equation

(eq 7) and the experimental data (continuous lines in Figure 5 and 6).

Table 3. **Best Fitting Values for the Thermal Inactivation Rate and Equilibrium Constants of Scheme 1 at 56.8 ºC**

Equilibrium constant	Best fitting value mM ± S.E.	Thermal inactivation rate constant	Best fitting value s^{-1} ± S.E.
K_k	0.18 ± 0.02	k_{ie}	$(15.2 \pm 0.8)\ 10^{-4}$
K_{K2}*	0.73 ± 0.07	k_{ieK}*	$(8.2 \pm 0.5)\ 10^{-4}$
K_{ATP}	0.009 ± 0.001	k_{ieK2}	$(1.4 \pm 0.2)\ 10^{-4}$
K_{ATPK}#	1.1 ± 0.1	k_{ieATP}	$(2.4 \pm 0.2)\ 10^{-4}$
K_{ATPK2}	7 ± 1	k_{ieATPK}*	$(15.2 \pm 0.8)\ 10^{-4}$
K_{KATP}	0.054 ± 0.005	$k_{ieATPK2}$*	$(1.4 \pm 0.2)\ 10^{-4}$
K_{K2ATP}#	0.5 ± 0.1		

The constants marked (*) were calculated assuming the constrained model described in the text, in which K_{K2}=4 K_K, k_{ieK}=(k_{ie}+k_{ieK2})/2, k_{ieATPK}=k_{ie} and $k_{ieATPK2}$=k_{ieK2}. The values of K_{ATPK}# and K_{K2ATP}# were calculated as $K_K.K_{KATP}/K_{ATP}$ and $K_{KATP}.K_{ATPK2}/K_{K2}$ respectively, using the thermodynamic equivalence of pathways, and propagating the error of the estimation of the fitted constants.

Some interesting consequences emerge from this analysis:

a) The equilibrium constants for the dissociation of ATP from the enzyme highly increase as

the enzyme progressively binds K^+ (i.e. $K_{ATP} < K_{KATP} < K_{K2ATP}$).

b) Binding of ATP to the enzyme produces a decrease in the affinity for K^+ since $K_K < K_{ATPK}$

and $K_{K2} < K_{ATPK2}$.

c) Binding of ATP to the free enzyme slows down the inactivation process ($k_{ie} > k_{ieATP}$), as it is

shown in Figure 2.

d) The inactivation rate constant decreases with binding of K^+ to the enzyme (i.e. $k_{ie} > k_{ieK} > k_{ieK2}$) in the absence of ATP (Figure 5A).

e) Binding of a single K^+ to the enzyme with ATP bound produces an increment of the inactivation rate constant since $k_{ieATP} < k_{ieATPK}$. Conversely, binding of a second K^+ diminishes 10 times the inactivation rate coefficient (i.e. $k_{ieATPK} > k_{ieATPK2}$).

Using the best fitting values of the equilibrium constants of Scheme 1 (Table 3) we simulated the fraction of the less stable species of the enzyme, calculated as ([E] + [EKATP])/[E]$_{total}$, at different ATP and K^+ concentrations (Figure S4A). The simulated curves present a biphasic dependence on K^+ concentration, quite similar to that observed for the dependence of k with [K^+] (cf. Figure S4A with Figure 5). The K^+ concentration at which the fraction of ([E] + [EKATP]) is maximum ([K^+]$_{max}$) increases as [ATP] rise. Remarkably, the values of K^+]$_{max}$ are not different to those corresponding to the maximum of k (Figure S4B). This supports the idea that, in the conditions tested, E and EKATP are the less stable species of the enzyme.

DISCUSSION

In this work we describe the effects of ATP, Mg^{2+} and K^+ on the thermal stability of the Na^+, K^+-ATPase. We observed that all structural and functional measurements vary along a single exponential function of time (eq 4). This simple behavior is indicative of a one-step process and appears to be common in P-ATPases, and another proteins,[48] even though it contrasts with the large size of the enzyme and its complex structural organization. [22,28,49–51]

Enzyme thermal inactivation is concomitant with conformational changes reflected by tryptophan fluorescence and a loss in ATP binding capacity detected by eosin-Y fluorescence, thus indicating a conformational rearrangement in the cytosolic domains where the ATP-binding

site is located. In addition, our previous results have shown that K^+ occlusion is also compromised.[29] However, despite the structural changes observed, complete inactivation of the pump is not accompanied by a major disorganization of its secondary structure as circular dichroism spectra does not change after the enzyme is fully inactivated.[52,29] These observations indicate that enzyme inactivation is the result of a small conformational change affecting both cytoplasmic and transmembrane domains.

ATP and Mg^{2+}, the main ligands of ATP binding domain of the pump, are shown to have a stabilizing effect against thermal inactivation (Figure 2). This effect could be explained by a change on the inactivation rate coefficient upon ligand binding as shown in Scheme 2. Note that in this scheme the inactive enzyme (E_i) could or not bind the ligand, and the inactivation reactions that lead to it are considered irreversible.

$$E \xrightleftharpoons{K_X} EX$$
$$E \xrightarrow{k_{ie}} E_i \xleftarrow{k_{ieX}} $$
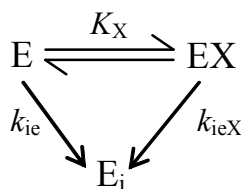
Scheme 2. Model of the interaction of the Na^+,K^+-ATPase with a ligand X.

K_X is the corresponding dissociation constant, while k_{ie} and k_{ieX} are the inactivation rate constants for the species E and EX respectively.

From this model and considering that ligand binding is in rapid equilibrium, the concentration of active enzyme decrease along a single exponential function of preincubation time where the apparent thermal inactivation rate coefficient (k_{app}) is a linear combination of k_{ie} and k_{ieX}

$$k_{app} = \frac{[E]}{[E]_{total}} k_{ie} + \frac{[EX]}{[E]_{total}} k_{ieX}$$

(8)

where $[E]/[E]_{total}$ and $[EX]/[E]_{total}$ are the fraction of free and ligand bound enzyme, respectively. In the absence of ligand, $[E]/[E]_{total} = 1$ and $[EX]/[E]_{total} = 0$ and then k_{app} will be equal to k_{ie}. Conversely, when $[X] \to \infty$, $[E]/[E]_{total} = 0$ and $[EX]/[E]_{total} = 1$ and $k_{app} = k_{ieX}$. Given that $K_X = [E] * [X] / [EX]$, $[E]_{total} = [E] + [EX]$ and $[X] >>> [Et]$, k_{app} will be:

$$k_{app} = \frac{k_{ie} K_X + k_{ieX} [X]}{K_X + [X]}$$

(9)

It can be seen that k_{app} vary with ligand concentration along a hyperbola from k_{ie} (at $[X]=0$) to k_{ieX} (at $[X] \to \infty$) where the $K_{0.5}$ of this function corresponds to the dissociation constant for the ligand (K_x).

Notice that this equation is equivalent to the empirical eq 5, whose coefficients k_0 and k_∞ can be reinterpreted as the inactivation rate constants of the free and fully bound enzyme (k_{ie} and k_{ieX} in Scheme 2, respectively). According to this model-derived equation the value of K_x is 7.3 ± 0.7 µM for ATP (at 56.8 °C) and 0.15 ± 0.02 mM for Mg^{2+} (at 58.5 °C). As expected, these values of K_x are 15-20 folds higher than those obtained at 25 ºC, 0.55 µM for ATP and 7.8 µM for Mg^{2+}.[47] Additionally, both K_x values are very low in respect to that corresponding to the ionic strength effect (12.7 ± 2.9 mM),[29] strongly suggesting that the effects of ATP and Mg^{2+} are a consequence of their specific effect on the enzyme.

Taking into account this analysis, enzyme inactivation experiments at several temperatures (Figure 3 and 4) were performed in the presence of ligand concentrations at least 10 times fold the corresponding K_X value. Due to that, the inactivation rate coefficients obtained can be assigned to the enzyme species with the ligand bound (k_{ieX} in Scheme 2). In this sense, at 56 ºC

the inactivation process of the enzyme species with Mg^{2+}, ATP or K^+ bound is 2.3, 7.7 or 26 times slower than that of the free enzyme (Table 1).

It has already been demonstrated that Na^+ specific binding causes destabilization of the enzyme upon thermal inactivation, whereas K^+ has the opposite effect exerted by the occlusion of this cation into the enzyme.[29] Considering that binding of Na^+ and K^+ changes the equilibrium distribution between the enzyme conformations leading towards E_1 and E_2 respectively,[53] it was postulated that E_1 conformation is less stable that E_2.[27-29] On the other hand, it is known that ATP and Mg^{2+} bind non covalently to the enzyme preferentially to the E_1 conformation.[47] In this work we show that the presence of either ATP or Mg^{2+} in the preincubation media stabilize the protein in the E1 conformation. A possible explanation for this apparent contradiction could be that the so-called E_1 conformation is not a unique state of the enzyme but a collection of states with some properties in common but other rather different. In the case of E2, comparison between the available atomic structures showed high degree of overall structural similarity despite potassium bound in the cation-binding sites.[18]

In this way, Mg^{2+} or ATP enzyme stabilization, in contrast with Na^+ effect, could be related to the cytoplasmic location of their binding sites, whereas Na^+ sites are located in the transmembrane region. Considering this, it is reasonable to hypothesize that cytoplasmic regions are more susceptible to thermal inactivation and become stabilized by ligand binding. Furthermore, this conjecture is consistent with the idea that transmembrane domains are more stable.[54,55] In apparent contradiction with this, K^+ binding to transmembrane sites on the Na^+,K^+-ATPase exerts a protective effect against thermal inactivation. However, in this case ion binding produces a change in the whole structure of the enzyme, including the cytosolic domains.[9,21]

Transition state analysis indicated that those ligands that bind to cytosolic domains diminish the activation entropy and enthalpy while, conversely, the magnitude of these parameters increase when K^+ is bound to the transmembrane region (Table 1). Also, ATP largely changes both entropic and enthalpic components suggesting a major reordering of the cytoplasmic domains in the transition state ($\Delta\Delta H^{\ddagger}$= -48 ± 8 kcal.mol^{-1} and $\Delta(T\Delta S^{\ddagger})$= -50 ± 8 kcal.mol^{-1}). A possible explanation for the differences observed in the thermodynamic activation parameters among Mg^{2+} and ATP is that the cation binds to P domain while the nucleotide promotes a more important structural rearrangement. Based on structural information from the sarco/endoplasmic reticulum Ca^{2+} ATPase, it is possible to postulate that the A domain rotates towards the phosphorylation site, interacting with both the P and N domains, leading to a more compact structure. In this sense, the unfavorable entropic effect ($\Delta(T\Delta S^{\ddagger})$) observed in the presence of ATP and in a small degree of Mg^{2+}, could be associated to a decrease in the conformational entropy of the transition state.

Even though the presence of ATP or K^+ in the preincubation media showed a clear stabilizing effect on the Na^+,K^+-ATPase (Figure 4), it can be observed that the simultaneous presence of both ligands does not have a synergistic effect. On the contrary, addition of ATP to preincubation media containing low K^+ concentration produces an increment on the enzyme thermal inactivation rate.

Based on the empirical analysis accomplished in this work, and previous information on the interaction of the Na^+,K^+-ATPase with both ATP and K^+,[47] a minimal model to explain the observed behavior was proposed (Scheme 1). According to this, the destabilizing component of the process can be attributed to the enzyme state generated by the simultaneous binding of one molecule of K^+ and ATP.

As previously postulated, K^+ protection of the enzyme against thermal inactivation can be attributed to the formation of occluded states of the enzyme. Thus, high thermal stability of the species $EATPK_2$ would be indicative of the occlusion of 2 K^+ ions even when ATP is bound to the enzyme while, on the other hand, the species EATPK would not have K^+ occluded. This assumption is in agreement with previous results which indicate that in Na^+,K^+-ATPase reaction cycle, ATP binding to $E(K_2)$ promotes the simultaneous release of both K^+ ions.[57] The decrease in enzyme affinity for ATP when K^+ is bound to the enzyme may account for a change in the interactions involved in nucleotide binding, and could explain the non protective effect observed.

ASSOCIATED CONTENT

SUPPORTING INFORMATION: Competition experiments between ATP and Eosin-Y for the binding to the Na^+, K^+-ATPase. Thermal inactivation rate coefficient as a function of [ATP] at different [K^+]. Meaning of the parameters of eq 6 in terms of ATP concentration and the equilibrium and thermal inactivation rate constants from Scheme 1. Best fitting values of the parameters of eq 6 as a function of ATP concentration. Thermal inactivation rate and less stable species correlation. (PDF)

AUTHOR INFORMATION

*E-mail: lolo@qb.ffyb.uba.ar

Tel: (+54 11) 49648289 (int. 131)

REFERENCES

1.   Skou, J. C.; Esmann, M. The Na,K-ATPase. *J. Bioenerg. Biomembr*. **1992**, *24*, 249–261.

2.   Hexum, T.; Samson, F. E.; Himes, R. H. Kinetic studies of membrane (Na^+-K^+-Mg^{2+})-ATPase. *Biochim. Biophys. Acta* **1970**, *212*, 322–331.

3.   Robinson, J. D. Nucleotide and divalent cation interactions with the (Na^++ K^+)-dependent ATPase. *Biochim. Biophys. Acta*. **1974**, *341*, 232–247.

4.   Møller, J. V.; Birte, J.; le Maire, M. Structural organization, ion transport, and energy transduction of P-type ATPases. *Biochim. Biophys. Acta* **1996**, *1286*, 1–51.

5.   Hasler, U.; Wang, X.; Crambert, G.; Béguin, P.; Jaisser, F.; Horisberger, J. D.; Geering, K. Role of beta-subunit domains in the assembly, stable expression, intracellular routing, and functional properties of Na,K-ATPase. *J. Biol. Chem*. **1998**, *273*, 30826–30835.

6.   Kühlbrandt, W.; Werner, K. Biology, structure and mechanism of P-type ATPases. *Nat. Rev. Mol. Cell Biol*. **2004**, *5*, 282–295.

7.   Morth, J. P.; Pedersen, B. P.; Toustrup-Jensen, M. S.; Sørensen, T. L. -M.; Petersen, J.; Andersen J. P.; Vilsen, B.; Nissen, P. Crystal structure of the sodium-potassium pump. *Nature* **2007**; *450*, 1043–1049.

8.   Shinoda, T.; Ogawa, H.; Cornelius, F.; Toyoshima, C. Crystal structure of the sodium-potassium pump at 2.4 A resolution. *Nature* **2009**, *459*, 446–450.

9.   Glynn, I. M.; Karlish, S. J. D. Occluded Cations in Active Transport. *Annu. Rev. Biochem.* **1990**, *59*, 171–205.

10.   Beaugé, L. A.; Glynn, I. M. Occlusion of K ions in the unphosphorylated sodium pump. *Nature* **1979**, *280*, 510–512.

11.   Esmann, M. Influence of Na on Conformational States in Membrane-Bound Renal Na,K-ATPase. *Biochemistry* **1994**, *33*, 8558–8565.

12.   Schneeberger, A.; Apell, H. J. Ion Selectivity of the Cytoplasmic Binding Sites of the Na,K-ATPase: I. Sodium Binding is Associated with a Conformational Rearrangement. *J. Membr. Biol.* **1999**, *168*, 221–228.

13.   Gonzalez-Lebrero, R. M.; Kaufman, S. B.; Montes, M. R.; Norby, J. G.; Garrahan, P. J.; Rossi, R. C. The Occlusion of Rb in the Na /K -ATPase: I. The identity of occluded states formed by the physiological or the direct routes: occlusion/deocclusion kinetics through the direct route. *J. Biol. Chem.* **2001**, *277*, 5910–5921.

14.   Forbush, B. The interaction of amines with the occluded state of the Na,K-pump. *J. Biol. Chem.* **1988**, *263,* 7979–7988.

15.   Rossi, R. C.; Nørby, J. G. Kinetics of K(+)-stimulated dephosphorylation and simultaneous K+ occlusion by Na,K-ATPase, studied with the K+ congener Tl+. The possibility of differences between the first turnover and steady state. *J. Biol Chem.* **1993**, *268*, 12579–12590.

16.   Robinson, J. D.; Pratap, P. R. Indicators of conformational changes in the Na /K -ATPase and their interpretation. *Biochim. Biophys. Acta* **1993**, *1154*, 83–104.

17.   Or, E.; Goldshleger, R.; Karlish, S. J. D. Characterization of disulfide cross-links between fragments of proteolyzed Na,K-ATPase: Implications for spatial organization of trans-membrane helices. *J. Biol. Chem.* **1999**, *274*, 2802–2809.

18.   Laursen, M.; Gregersen, J. L.; Yatime, J.; Nissen, P.; Fedosova, N. U. Structures and characterization of digoxin- and bufalin-bound Na^+,K^+-ATPase compared with the ouabain-bound complex. *Proc. Natl. Acad. Sci. U.S.A.* **2014**, *112*, 1755–1760

19.   Apell, H. J.; Karlish, S. J. Functional properties of Na,K-ATPase, and their structural implications, as detected with biophysical techniques. *J. Membr. Biol.* **2001**, *180*, 1–9.

20.   Kaplan, J. H. Biochemistry of Na,K-ATPase. *Annu. Rev. Biochem.* **2002**, *71*, 511–535.

21.   Horisberger, J. D. Recent insights into the structure and mechanism of the sodium pump. *Physiology (Bethesda)* **2004**, *19*, 377–387.

22.   Jørgensen, P. L.; Andersen, J. P. Thermoinactivation and aggregation of alpha beta units in soluble and membrane-bound (Na,K)-ATPase. *Biochemistry* **1986**, *25*, 2889–2897.

23.   Goldshleger, R.; Tal, D. M.; Karlish, S. J. Topology of the alpha-subunit of Na,K-ATPase based on proteolysis. Lability of the topological organization. *Biochemistry* **1995**, *34* 8668–8679.

24.   Shainskaya, A.; Nesaty, V.; Karlish, S. J. Interactions between fragments of trypsinized Na,K-ATPase detected by thermal inactivation of Rb^+ occlusion and dissociation of the M5/M6 fragment. *J. Biol. Chem.* **1998**, *273*, 7311–7319.

25.   Grinberg, A. V.; Gevondyan, N. M.; Grinberg, N. V.; Grinberg, V. Y. The thermal unfolding and domain structure of Na^+/K^+-exchanging ATPase. A scanning calorimetry study. *Eur. J. Biochem.* **2001**, *268*, 5027–5036.

26.   Donnet, C.; Arystarkhova, E.; Sweadner, K. J. Thermal denaturation of the Na,K-ATPase provides evidence for alpha-alpha oligomeric interaction and gamma subunit association with the C-terminal domain. *J. Biol. Chem.* **2001**, *276*, 7357–7365.

27.   Fischer, T. H. The effect of Na^+ and K^+ on the thermal denaturation of Na^+ and K^+-dependent ATPase. *Biochem. J.* **1983**, *211*, 771–774.

28.   Fodor, E.; Fedosova, N. U.; Ferencz, C.; Marsh, D.; Pali, T.; Esmann, M. Stabilization of Na,K–ATPase by ionic interactions. *Biochim. Biophys. Acta* **2008**, *1778*, 835–843.

29.   Kaufman, S. B.; González-Flecha, F. L.; González-Lebrero, R. M. Opposing effects of Na^+ and K^+ on the thermal stability of Na^+,K^+-ATPase. *J. Phys. Chem. B* **2012**, *116*, 3421–3429.

30.   Jorgensen, P. L. Purification and characterization of $(Na^+$ plus $K^+)$-ATPase. 3. Purification from the outer medulla of mammalian kidney after selective removal of membrane components by sodium dodecylsulphate. *Biochim. Biophys. Acta* **1974**, *356*, 36–52.

31.   Klodos, I.; Esmann, M.; Post, R. L. Large-scale preparation of sodium-potassium ATPase from kidney outer medulla. *Kidney Int.* **2002**, *62*, 2097–2100.

32.   Baginski, E. S.; Foa, P. P.; Zak, B. Determination of phosphate: Study of labile organic phosphate interference. *Clin. Chim. Acta* **1967**, *15*, 155–158.

33.   Incicco, J. J.; Gebhard, L. G.; González-Lebrero, R. M.; Gamarnik, A. V.; Kaufman, S.B. Steady-State NTPase Activity of Dengue Virus NS3: Number of Catalytic Sites, Nucleotide Specificity and Activation by ssRNA. *PLoS One* **2013**, *8*, e58508.

34.   Hagen, S. J. Solvent viscosity and friction in protein folding dynamics. *Curr. Protein Pept. Sci.* **2010**, *11*, 385–395.

35.   Hänggi, P.; Peter, H.; Peter, T.; Michal, B. Reaction-rate theory: Fifty years after Kramers. *Rev. Mod. Phys.* **1990**, *62*, 251–341.

36.   Kramers, H. A. Brownian motion in a field of force and the diffusion model of chemical reactions. *Physica* **1940**, *7*, 284–304.

37.   Ansari, A.; Jones, C. M.; Henry, E. R.; Hofrichter, J.; Eaton, W. A. The role of solvent viscosity in the dynamics of protein conformational changes. *Science* **1992**, *256*, 1796–1798.

38.   Noronha, M.; Gerbelová, H.; Faria, T. Q.; Lund, D. N.; Smith, D. A.; Santos, H.; Maçanita, L. M. Thermal unfolding kinetics of ubiquitin in the microsecond-to-second time range probed by Tyr-59 fluorescence. *J. Phys. Chem. B* **2010**, *114*, 9912–9919.

39.   Gavish, B. Molecular dynamics and the transient strain model of enzyme catalysis. In *The fluctuating enzyme*; G Rickey Welch, Ed.; Wiley: New York, **1986.**

40.   Zhu, Y.; Alonso, D. O. V.; Maki, K.; Huang, C. –Y.; Lahr, S. J.; Daggett, V.; Roders, H.; DeGrado, W. F.; Gai, F. Ultrafast folding of alpha3D: A de novo designed three-helix bundle protein. *Proc. Natl. Acad. Sci. U.S.A.* **2003**, *100*, 15486–15491.

41.   Torrent, J.; Marchal, S.; Ribó, M.; Vilanova, M.; Georges, C.; Dupont, Y.; Lange, R. Distinct unfolding and refolding pathways of ribonuclease A revealed by heating and cooling temperature jumps. *Biophys. J.* **2008**, *94*, 4056–4065.

42.   Yamaoka, K.; Nakagawa, T.; Uno, T. Application of Akaike's information criterion (AIC) in the evaluation of linear pharmacokinetic equations. *J. Pharmacokinet. Biopharm.* **1978**, *6*, 165–175.

43.   Ladokhin, A. S.; Jayasinghe, S.; White, S. H. How to measure and analyze tryptophan fluorescence in membranes properly, and why bother? *Anal. Biochem.* **2000**, *285*, 235–245.

44.   Skou, J. C.; Esmann, M. Eosin, a fluorescent probe of ATP binding to the $(Na^+ + K^+)$-ATPase. *Biochim. Biophys. Acta* **1981**, *647*, 232–240.

45.   Skou, J. C.; Esmann, M. Eosin as a fluorescence probe for measurement of conformational states of Na$^+$,K$^+$-ATPase. *Methods Enzymol* **1988**, *156*, 278-281.

46.   Jørgensen, P. L.; Andersen, J. P. Thermoinactivation and aggregation of alpha beta units in soluble and membrane-bound (Na,K)-ATPase. *Biochemistry* **1986**, *25*, 2889–2897.

47.   Gonzalez-Lebrero, R. M.; Kaufman, S. B.; Garrahan, P. J.; Rossi, R. C. The Occlusion of Rb$^+$ in the Na$^+$/K$^+$-ATPase. II. The effects of Rb$^+$, Na$^+$, Mg^{2+}, or ATP on the equilibrium between free and occluded Rb$^+$. *J. Biol. Chem.* **2002**, *277*, 5922–5928.

48.   Sanchez-Ruiz, J. M. Protein kinetic stability. *Biophys. Chem.* **2010**, *148*, 1-15

49.   Levi, V.; Rossi, J. P. F. C.; Echarte, M. M.; Castello, P. R.; González Flecha, F. L. Thermal stability of the plasma membrane calcium pump. Quantitative analysis of its dependence on lipid-protein interactions. *J. Membr. Biol.* **2000**, *173*, 215–225.

50.   Cattoni, D. I.; González Flecha, F. L.; Argüello, J. M. Thermal stability of CopA, a polytopic membrane protein from the hyperthermophile Archaeoglobus fulgidus. *Arch. Biochem. Biophys.* **2008**, *471*, 198–206.

51.   Fischer, T. H. The effect of Na$^+$ and K$^+$ on the thermal denaturation of Na+ and + K+-dependent ATPase. *Biochem. J.* **1983**, *211*, 771–774.

52.   Miles, A. J.; Wallace, B. A.; Esmann, M. Correlation of structural and functional thermal stability of the integral membrane protein Na,K-ATPase. *Biochim. Biophys. Acta* **2011**, *1808*, 2573–2580.

53.   Esmann, M. Influence of Na+ on conformational states in membrane-bound renal Na,K-ATPase. *Biochemistry* **1994**, *33*, 8558–8565.

54.   Haltia, T.; Freire, E. Forces and factors that contribute to the structural stability of membrane proteins. *Biochim. Biophys. Acta* **1995**, *1241*, 295–322.

55.   Roman, E. A.; González Flecha, F. L. Kinetics and thermodynamics of membrane protein folding. *Biomolecules* **2014**, *4*, 354–373.

56.   Møller, J. V.; Olesen, C.; Winther, A. M. L.; Nissen, P. The sarcoplasmic Ca^{2+}-ATPase: design of a perfect chemi-osmotic pump. *Q. Rev. Biophys.* **2010**, *4*, 501–566.

57.   Kaufman, S. B.; González-Lebrero, R. M.;, Schwarzbaum, P. J.; Nørby, J. G.; Garrahan, P. J.; Rossi, R. C. Are the States That Occlude Rubidium Obligatory Intermediates of the Na$^+$/K$^+$-ATPase Reaction? *J. Biol. Chem.* **1999**, *274*, 20779-20790.

1
2
3
4
5
6
7
8
9
10
11
12
13
14
15
16
17
18
19
20
21
22
23
24
25
26
27
28
29
30
31
32
33
34
35
36
37
38
39
40
41
42
43
44
45
46
47
48
49
50
51
52
53
54
55
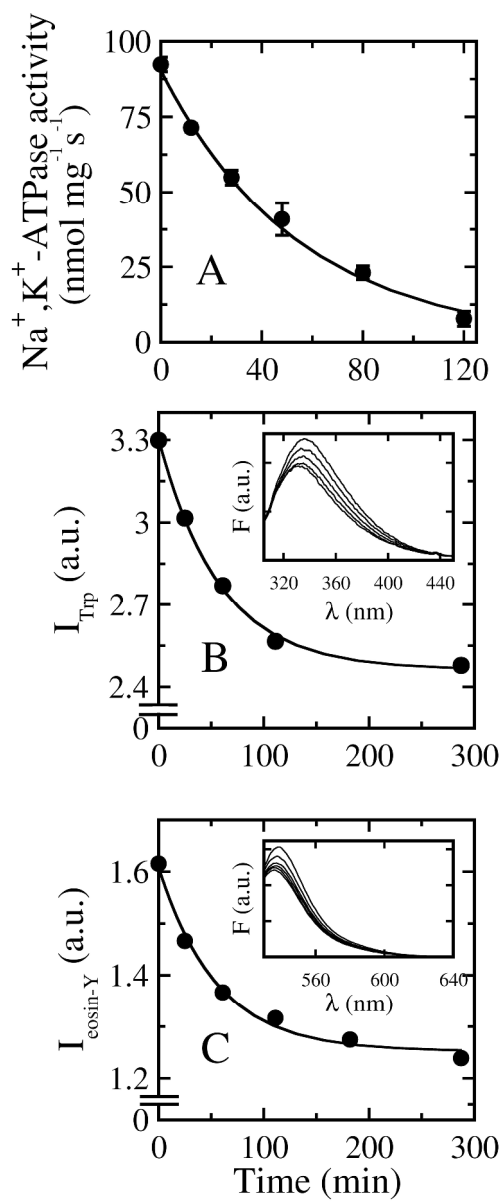56
57
58
59
60

TOC GRAPHIC
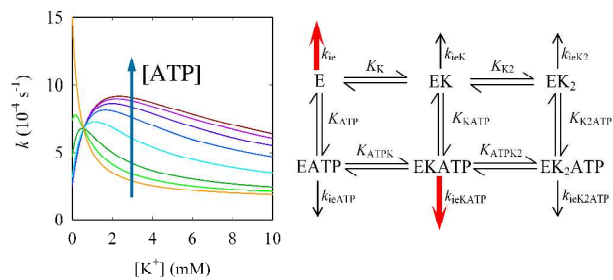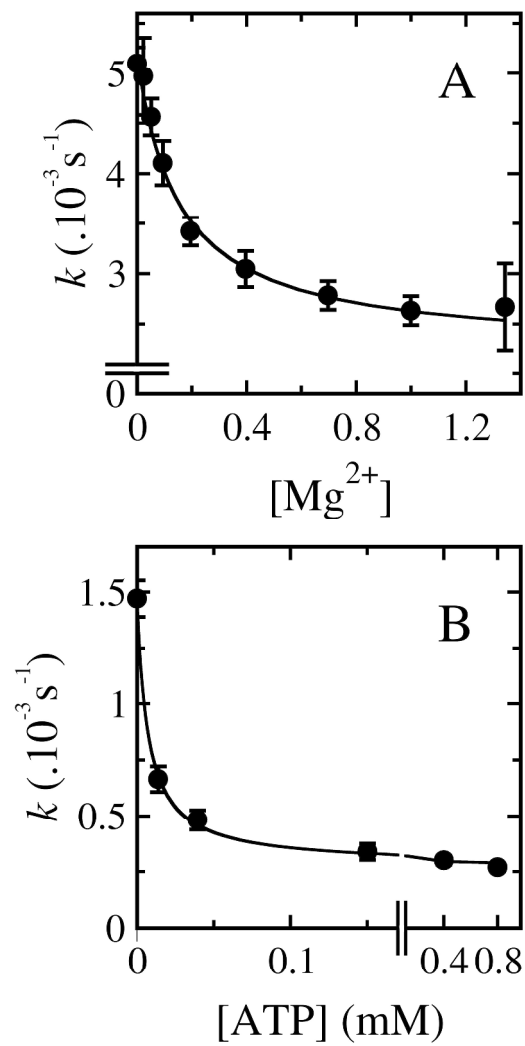
Figure 1

168x404mm (600 x 600 DPI)
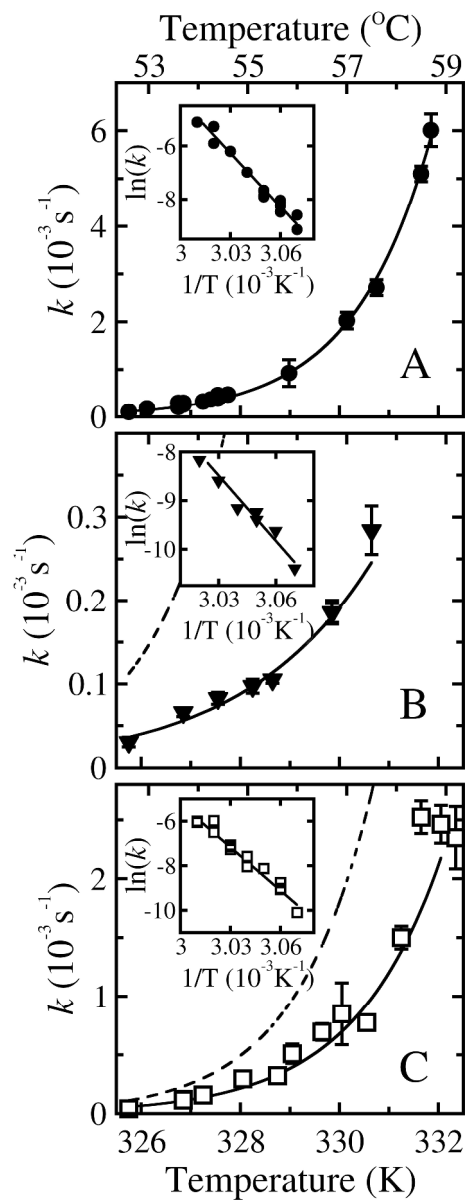
Figure 2

142x267mm (600 x 600 DPI)

Figure 3

157x354mm (600 x 600 DPI)

Figure 4

133x255mm (600 x 600 DPI)

1
2
3
4
5
6
7
8
9
10
11
12
13
14
15
16
17
18
19
20
21
22
23
24
25
26
27
28
29
30
31
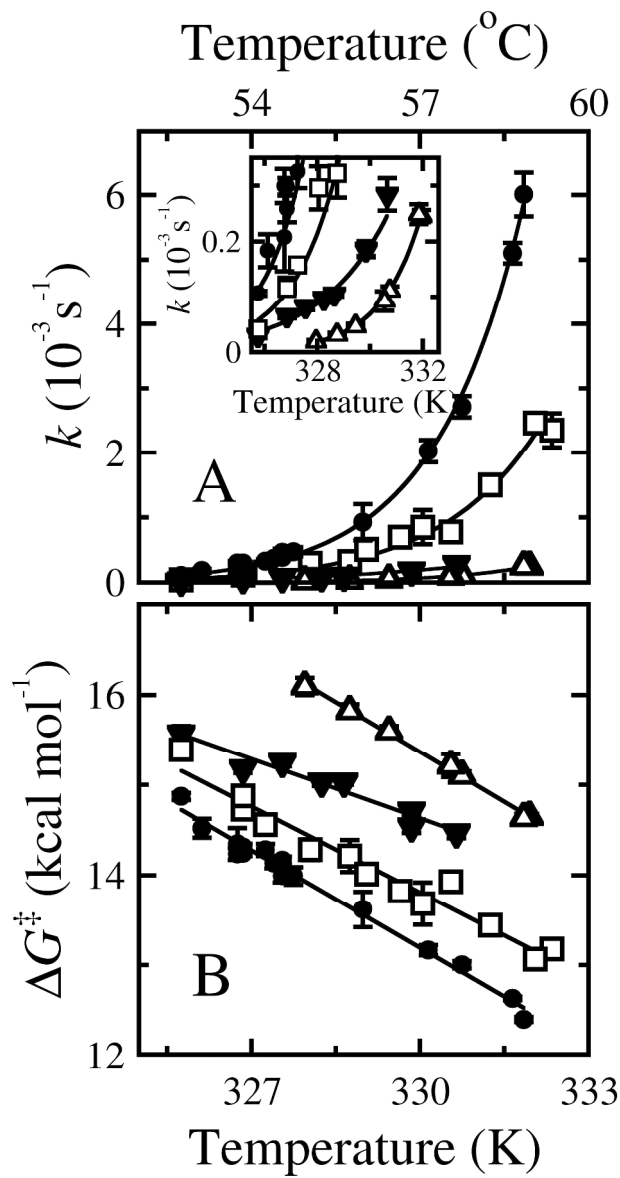32
33
34
35
36
37
38
39
40
41
42
43
44
45
46
47
48
49
50
51
52
53
54
55
56
57
58
59
60

Unable to Convert Image

The dimensions of this image (in pixels) are too large
to be converted. For this image to convert,
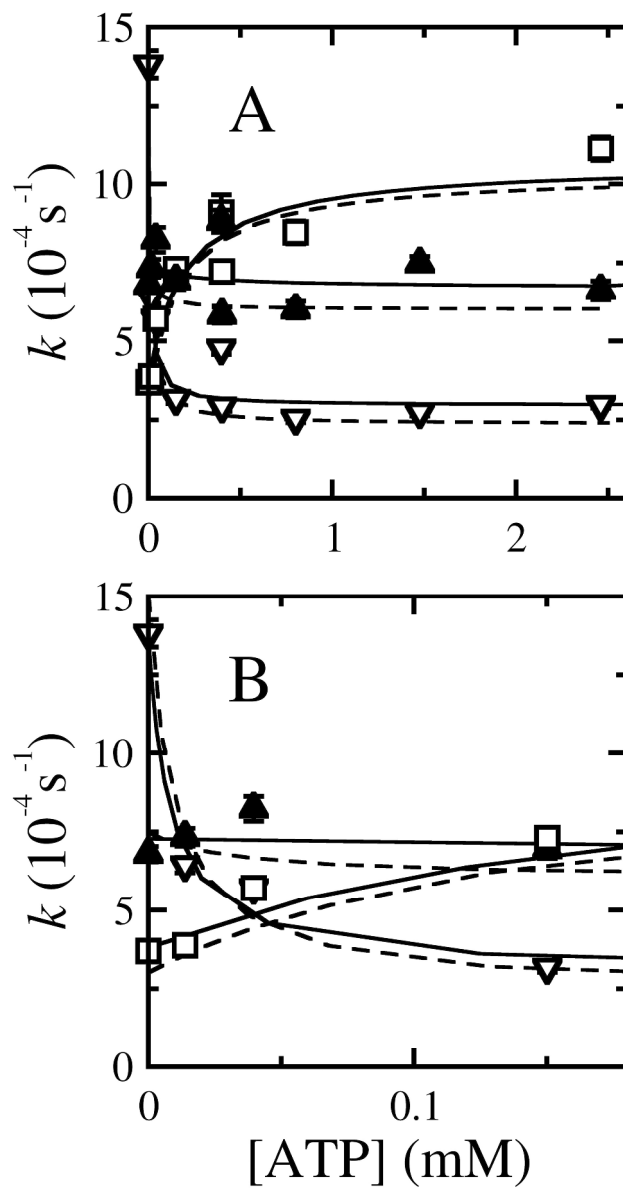the total number of pixels (height × width) must be
less than 40,000,000 (40 megapixels).

Figure 5

Figure 6

132x251mm (600 x 600 DPI)